

2010

# Tuning $\sigma$ -Holes: Charge Redistribution in the Heavy (Group 14) Analogues of Simple and Mixed Halomethanes Can Impose Strong Propensities for Halogen Bonding

Kelling J. Donald

*University of Richmond*, [kdonald@richmond.edu](mailto:kdonald@richmond.edu)

Bernard K. Wittmaack

Chad Crigger

Follow this and additional works at: <http://scholarship.richmond.edu/chemistry-faculty-publications>

 Part of the [Other Chemistry Commons](#)

## Recommended Citation

Donald, Keilling J., Bernard K. Wittmaack, and Chad Crigger. "Tuning  $\sigma$ -Holes: Charge Redistribution in the Heavy (Group 14) Analogues of Simple and Mixed Halomethanes Can Impose Strong Propensities for Halogen Bonding." *Journal of Physical Chemistry* 114, no. 26 (2010): 7213-7222. doi:10.1021/jp102856v.

This Article is brought to you for free and open access by the Chemistry at UR Scholarship Repository. It has been accepted for inclusion in Chemistry Faculty Publications by an authorized administrator of UR Scholarship Repository. For more information, please contact [scholarshiprepository@richmond.edu](mailto:scholarshiprepository@richmond.edu).

# Tuning $\sigma$ -Holes: Charge Redistribution in the Heavy (Group 14) Analogues of Simple and Mixed Halomethanes Can Impose Strong Propensities for Halogen Bonding

Kelling J. Donald,\* Bernard K. Wittmaack, and Chad Crigger

Department of Chemistry, Gottwald Center for the Sciences, University of Richmond,  
Richmond, Virginia 23173

Received: March 30, 2010; Revised Manuscript Received: May 11, 2010

Halogen bonding between halide sites (in substituted organic molecules or inorganic halides) and Lewis bases is a rapidly progressing area of exploration. Investigations of this phenomenon have improved our understanding of weak intermolecular interactions and suggested new possibilities in supramolecular chemistry and crystal engineering. The capacity for halogen bonding is investigated at the MP2(full) level of theory for 100 compounds, including all 80  $MH_{4-n}X_n$  systems ( $M = C, Si, Ge, Sn, \text{ and } Pb$ ;  $X = F, Cl, Br, \text{ and } I$ ). The charge redistribution in these molecules and the (in)stability of the  $\sigma$ -hole at X as a function of M and  $n$  are catalogued and examined. For the mixed  $MH_{3-m}F_mI$  compounds, we identify a complicated dependence of the relative halogen bond strengths on M and  $m$ . For  $m = 0$ , for example, the  $H_3C-I\cdots NH_3$  halogen bond is 6.6 times stronger than the  $H_3Pb-I\cdots NH_3$  bond. When  $m = 3$ , however, the  $F_3Pb-I\cdots NH_3$  bond is shorter and  $\sim 1.6$  times stronger than the  $F_3C-I\cdots NH_3$  bond. This substituent-induced reversal in the relative strengths of halogen bond energies is explained.

## 1. Introduction

Carbon is an exceptional element in many ways. The study of organic compounds is a special category in modern chemistry because the chemistry of carbon is very different from that of the heavier group 14 congeners. The decreasing penchant for multiple bonding and catenation going down group 14 are cases in point. Even in relatively simple systems, such as the one-, or two-carbon alkanes and haloalkanes, the thermodynamic stability and reactivity of the compounds are radically modified if we replace the carbon atom(s) by Si, Ge, Sn, or Pb.<sup>1</sup>

The series of small ternary  $MH_{4-n}X_n$  molecules ( $M = C, Si, Ge, Sn, \text{ and } Pb$ ;  $X = F, Cl, Br, \text{ and } I$ ) illustrates well the diversity in the bonding and the divergent biological and industrial applications of simple carbon compounds and their group 14 analogues. The halomethanes ( $M = C$ ) find use as solvents and reagents in chemical laboratories and have applications in medicine, agriculture, and other industries. Several of the halosilanes and halogermanes find use in synthetic processes,<sup>2</sup> and as starting materials in the preparation of high purity components in the manufacture of semiconductors and other electronic devices.<sup>3,4</sup> In synthetic chemistry, the halostannanes are useful reagents in organotin synthesis and catalysts.<sup>5</sup> Use of Pb(IV) compounds is not as widespread; the divalent species Pb(II) is far more common and, of course, it does not help that lead compounds can be quite toxic.<sup>5</sup>

In a series of two papers<sup>6,7</sup> one of us and co-workers examined the structure and bonding in several of the halomethanes, -silanes and -germanes ( $MH_{4-n}X_n$ ;  $X = F, Cl, Br$ ). In those contributions, our objective was to understand better the competing (attractive and repulsive) interactions that account for anomalous variations in geometrical, and electronic properties of these molecules. An  $M-X$  bond elongation that occurs as  $n$  increases in the chloro- and bromomethanes was identified and rationalized.<sup>8</sup> A model

was proposed as well to explain variations in the charge distribution in the  $MH_{4-n}X_n$  molecules as functions of  $n$ .

In this report, we extend our investigation to include the computationally more demanding halostannane and haloplumbane systems ( $MH_{4-n}X_n$ ,  $n = 1-4$ ;  $M = Sn, \text{ and } Pb$ ;  $X = F, Cl, Br, \text{ and } I$ ). Since a more demanding (MP2(full)) model chemistry has been employed in this contribution (see Methods section below), the complete series of eighty ternary halomethane compounds,  $MH_{4-n}X_n$  ( $M = C, Si, Ge, Sn, \text{ and } Pb$ ), has been systematically (re)examined. In addition to our current treatment of the Sn and Pb systems, the iodides,  $MH_{4-n}I_n$ ,—which have not been considered previously, even for  $M = C, Si, \text{ or } Ge$ <sup>6,7</sup>—are included in this work. To be sure, we want to deepen our understanding of the influence of halogenation on the charge distribution in molecules. However, our larger objective in this contribution is to examine in detail the propensities for halogen bonding by the simple and mixed halomethanes and their group 14 analogues. In this quest, we consider briefly the reliability of simple computational parameters (such as the natural bond orbital<sup>9</sup> (NBO) charge separations in the  $M-X$  bond, and the (s-p) hybrid orbital compositions at the X) as predictors of the relative strengths of halogen bonds.

**Halogen Bonding.** The group of halomethanes is a practical test set for studying the nature of halogen bonding interactions. The general class of interactions described as halogen bonds (abbreviated X-bonds) are weak bonding interactions (Figure 1) between (i) a polarizable halogen atom, X, in a molecular species  $R-X$ , (e.g., I in  $F_3C-I$ ) that acts as the Lewis acid and (ii) a nucleophilic atomic site, Y (such as O, N, or S, for example), in a neighboring molecular species ( $Y-R'$ ). The strength of the X-bond ( $R-X\cdots Y-R'$ ) varies widely (from  $<0.5$  kcal/mol (0.02 eV) to  $>40$  kcal/mol (1.7 eV)),<sup>10,11</sup> such that an X-bond may be even stronger than some hydrogen bonds.<sup>10,12</sup> In general, the halogen bond strength increases as X becomes more polarizable ( $I > Br > Cl \gg F$ ), and as Y becomes more nucleophilic.<sup>11,13</sup> Halogen bonds with  $X = F$  have been identified in some cases where R is very strongly electron withdrawing,

\* Corresponding Author: Telephone: 804-484-1628. Fax: 804-287-1897; E-mail: kdonald@richmond.edu.

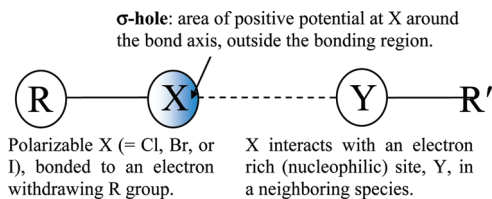


**Figure 1.** Depiction of halogen bonding in which the halogen atom, X, is bonded covalently to an atom or group, R, and interacts with an electron-rich site Y (such as O, N, or S) on a neighboring Lewis base (Y–R').

but such R–F---Y–R' bonds are exceptionally weak compared to the other X-bonds.<sup>14</sup>

These interactions have come to be called halogen bonds,<sup>15</sup> owing to the obvious analogy to hydrogen bonds (R–H---Y–R'),<sup>11,16,17</sup> and have been observed experimentally for several decades.<sup>18,19</sup> They are commonly encountered as charge-transfer or donor–acceptor interactions in the literature before 1980,<sup>15–19</sup> and are typified by unusually short X---Y interatomic separations (shorter than the sum of the van der Waals radii of X and Y).<sup>17b,20</sup> A resurgence of interest in these X-bonding interactions has been spurred by mounting evidence of their biological relevance,<sup>21,22</sup> and potential applications in crystal engineering.<sup>10–12,23,24</sup>

In ref 11, Politzer et al. explain in detail how an (s-p) hybridization of the X orbital that is involved in the R–X bond can give rise to a significant charge depletion at X outside the R–X bonding region. This charge deficient zone—the so-called  $\sigma$ -hole—is characterized by a positive electrostatic potential. Using the haloalkanes (CH<sub>3–n</sub>F<sub>n</sub>X (X = Cl, Br, I; n = 1, 2, and 3)) as their sample set, Politzer et al. showed that, for a given n, the stability and size of the  $\sigma$ -hole increases as X becomes less electronegative: the hole is absent or very small for X = F,<sup>14</sup> but appears and expands going down group 17 from X = Cl to X = I.<sup>11,25</sup> Moreover, they identified a link between the participation of the filled ns orbital (%s contribution) in the hybrid orbital at X in the R–X bond and the size of the  $\sigma$ -hole. They showed that, for a given X atom, significant ns–np mixing leads to an influx of electron density into the X hybrid orbital and shrinkage of the  $\sigma$ -hole.

Conversely, a low %s contribution (or a very electronegative R group), increases the charge deficiency at X along the R–X bond axis, and magnifies the  $\sigma$ -hole. This enlargement of the size and electrophilicity (or strength)<sup>26</sup> of the  $\sigma$ -hole at X going down group 17 is responsible for an observed increase in the X-bond energy as X gets larger. Now,  $\sigma$ -holes are, of course, not exclusive to halogens. Since the identification of the  $\sigma$ -hole at halide sites in halomethanes,<sup>25</sup> analogous forms of “ $\sigma$ -hole bonding”<sup>17a,27</sup> have been identified in which a Lewis base interacts with a  $\sigma$ -hole on a covalently bonded atom from elsewhere in the periodic table (such as group 14,<sup>28,29</sup> 15,<sup>30</sup> or 16<sup>31</sup>).

It would be quite useful indeed to have a simple parameter that enabled us to estimate the relative strength of  $\sigma$ -holes in a series of R–X molecules with different R groups, for example. A question that we touch upon is whether either point charges or hybrid orbital compositions at X may be used to gauge the relative strengths of halogen bonds for different R–X molecules.

To be sure, point charge models that assign a single net charge to each atom in a molecule are of no utility in rationalizing the directionality of X-bonds, or quantifying the strength of the bonds.<sup>32,33</sup> Nonetheless, since the halide, X, is a terminal atom bonded to a single site in R, (primarily via a single hybrid orbital), it is plausible that the larger the charge transfer along the bond axis from X toward R, (hence the less negative the

net charge at X,  $q_X$ , becomes), the larger the  $\sigma$  hole at X will be. For the CF<sub>3</sub>X compounds, for example, the  $\sigma$ -hole is largest for X = Br and I, and the computed NBO point charges at X are actually positive ( $q_{Br} = 0.04e$ ;  $q_I = 0.11e$ ).<sup>34</sup> A similar positivation at Br and I in the CH<sub>4–n</sub>Br<sub>n</sub> and CH<sub>4–n</sub>I<sub>n</sub> systems, respectively, has been reported in ref 6 as well.

Politzer et al. have provided substantial evidence that the degree of hybridization (%s composition) at the X orbital in the C–X bond is a chemically meaningful, accessible, and reliable predictor of the propensity for halogen bonding.<sup>34</sup> This connection between the  $\sigma$ -hole strength and the X orbital composition is confirmed here for M = C and is demonstrated for the first time for the Si, Ge, Sn, and Pb halomethanes analogues, as well. We caution, however, against any cross-comparison of the orbital compositions at identical X sites bonded to different M atoms. We find that such comparisons are invalid as strategies for predicting the relative strengths of the  $\sigma$ -holes or the actual X-bond energies. Halogen bond energies for a series of MH<sub>3–m</sub>F<sub>m</sub>I molecules examined in this report show for the first time that X-bonds formed by C species may be weaker than X-bond formed by some of their heavier inorganic analogues.

## 2. Computational Methods

All the results reported in this work have been obtained at the Møller–Plesset (MP2(full)) level of theory.<sup>35</sup> These data include the optimized geometries of all the molecules studied, the computed NBO point charges and orbital hybridization data (all obtained from a natural bond orbital analysis on the MP2 densities), and the iso-density surfaces plus the associated electrostatic potentials for several cases. The 6-311+G\* basis sets<sup>36</sup> have been employed for H and the lighter elements in both groups 14 and 17: M = C, Si, Ge, and X = F, Cl, Br. For the computationally more demanding cases, M = Sn, Pb, and X = I, we used scalar-relativistic energy-consistent small core Dirac–Fock (MDF) effective-core pseudopotentials (ECPs): 28e<sup>–</sup> cores for Sn and I, and a 60e<sup>–</sup> core for Pb (without the spin–orbit potential but including the scalar relativistic effects), and the corresponding (MDF cc-pVTZ-pp) basis sets.<sup>37</sup> All ab initio calculations were performed using the Gaussian 03 suite of programs.<sup>38</sup> The orbital pictures and electrostatic potential representations have been generated using the GaussView graphics software.<sup>39</sup>

## 3. Results and Discussion

**3.1. Geometry and Charge Distribution.** The computed MP2(full) geometrical parameters obtained for the halostannanes and haloplumbanes are shown in Table S.1a of the Supporting Information. Experimental data are scarce for these molecules, but they are included where available.<sup>40,41</sup> For the halomethanes, -silanes, and -germanes,—for most of which computed geometries were published previously<sup>6,7</sup>—the updated MP2(full) structural parameters are listed in Table S.1b.<sup>42,43</sup>

The bulk of our attention will be focused on the charge distribution in the halomethanes and their Si, Ge, Sn, and Pb analogues rather than the geometrical trends, which have been highlighted in refs 6 and 7 for most of the C, Si, and Ge systems. We are pleased, however, that the computed geometries in Tables S.1a,b show very good agreement with experiment. Perhaps the most remarkable feature of the structural data for the stannanes and plumbanes is the relatively small separation between the Sn–X and Pb–X (and the Sn–H and Pb–H) bonds.<sup>44</sup>

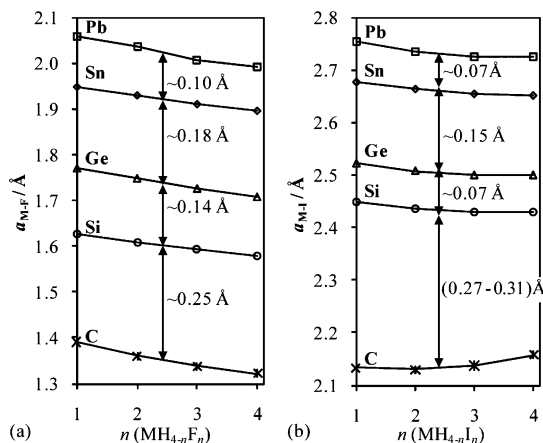


**Figure 2.** Differences in the (a) M–F and (b) M–I bond distances in the  $MH_{4-n}X_n$  molecules,  $n = 1 - 4$ ;  $M = C, Sn, Ge, Sn, Pb$ .

The comprehensive series of plots in Figure 2 for  $X = F$  and  $I$  shows that the difference between the Sn–X and Pb–X bond is never larger than  $\sim 0.10$  Å and highlights a similar situation going from the Si to the Ge systems.

The irregular spacing of the lines in Figure 2, in particular the small differences in  $a_{M-X}$  for the Sn versus Pb (and Si vs Ge) compounds, mirror the well-known consequences of periodicity on the atomic radii of the elements (the group 14, M, atoms, in this case).<sup>45–47</sup> The relatively small atomic radii of Ge and Pb are explained very well by the influence of the so-called d-orbital and lanthanide contractions<sup>48</sup> on elements in periods 4 and 6, respectively. For Pb, and the period 6 elements in general, relativistic effects contribute to the contraction in the ground state radii, as well.<sup>46</sup> We see in the next sections

that relativistic effects, by influencing atomic properties (such as the polarizabilities) of Pb, are decisive for the strength of the X-bonds formed by the haloplumbanes.

**3.1.1. Charge Distribution in  $MH_{4-n}X_n$ :  $M = C$  is the Exception, Not the Rule.** We set the basis for an assessment of the  $\sigma$ -holes at X in the  $MH_{4-n}X$  compounds with a brief but comprehensive discussion of the charge distribution in these molecules. The computed NBO charges for the central atoms, M, and the halide atoms, X, are summarized in Figures 3a and 3b respectively.

Several general patterns emerge when we compare the two sets of plots in Figure 3. Importantly, the charge distribution in the halomethane molecules ( $M = C$ ) is very different from what we observe for the Si, Ge, Sn, and Pb compounds. For any X and n, the carbon centers are far more negative than the other M sites (Figure 3a). Put another way, only a relatively small fraction of the charge density of the carbon atom is transferred to the halides, so the X sites that are bonded to C are far less negative than they are in the heavier systems (Figure 3b). The situation is especially remarkable for the iodomethanes where the NBO charges at I,  $q_I$ , are all positive. Here, however, we are primarily interested in the qualitative observation that  $q_X$  is significantly more positive when bonded to  $M = C$  compared to the other ( $M \neq C$ ) cases (see the large gap between the  $M = C$  and  $M \neq C$  systems in Figure 3b); we will not be concerned with the actual magnitude of the individual charges per se.

**3.1.2. Electronegativity and Charge Distribution.** The clustering of the Si, Ge, Sn, and Pb curves in the positive region of Figure 3a shows clearly that (for  $X = F$  in particular) the charge shift along the M–X bond, for all  $M \neq C$ , is quite insensitive to the identity of M. So, why are the carbon systems so different? The very low polarizability<sup>49</sup> (and noticeably higher

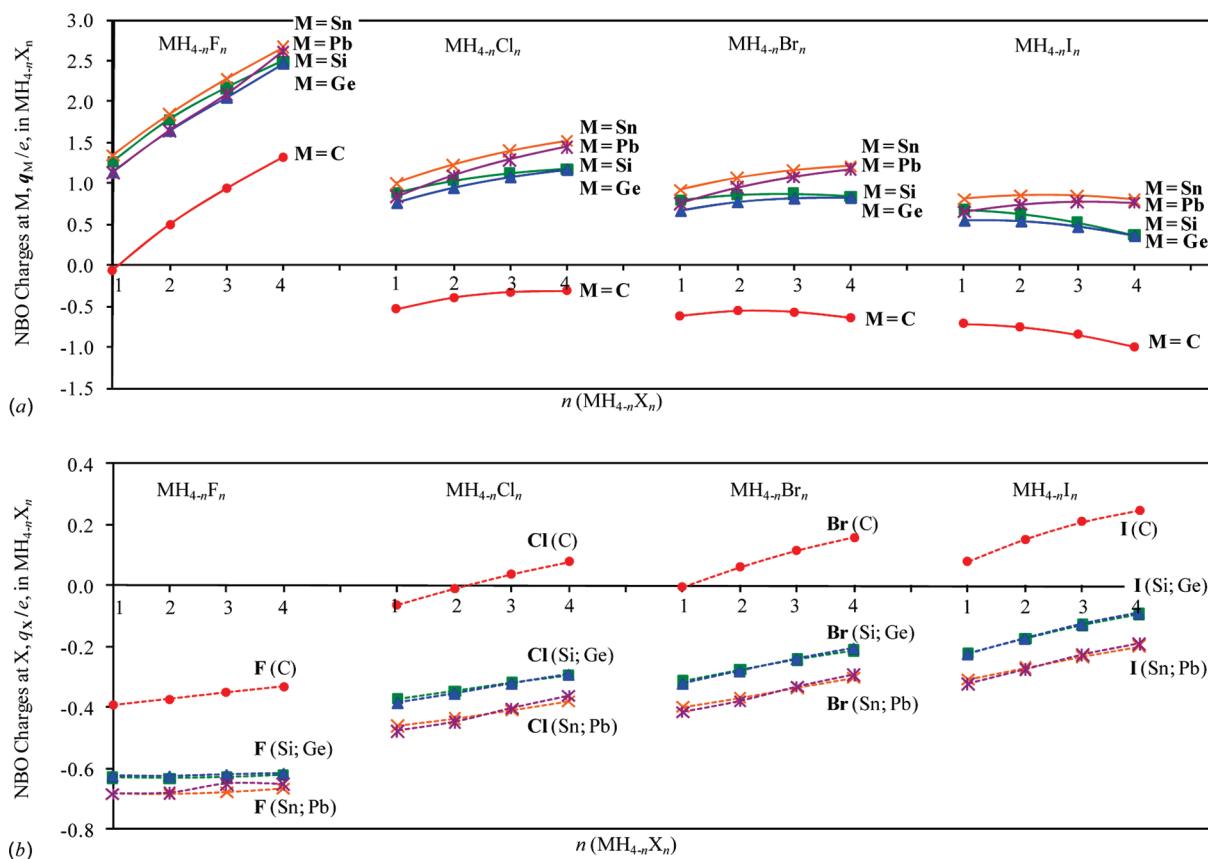


**Figure 3.** NBO point charges for (a) the central atoms,  $q_M$ , and (b) the halides,  $q_X$ , in the  $MH_{4-n}X_n$  molecules. The  $q_M$  and  $q_X$  data plotted above and the corresponding  $q_H$  values are all provided in Tables S.2(a–e) in the Supporting Information.

**TABLE 1: Covalent Radii ( $r$ ), Ground State Polarizabilities ( $\alpha^{(GS)}$ , in volume units), and Pauling and (Mulliken) Absolute Ground State and  $sp^3$  (tetrahedral) Valence State Electronegativities ( $\chi^P$ ,  $\chi^{M(GS)}$ , and,  $\chi^{M(vS)(tet)}$ , Respectively) of Groups 14 and 17 Elements<sup>a</sup>**

	$r$ , Å	$\alpha^{(GS)}$ , Å <sup>3</sup>	electronegativities		
			$\chi^P$	$\chi^{M(GS)}$ , eV	$\chi^{M(vS)(tet)}$ , eV
C	0.75	1.76	2.55	6.27	8.15
Si	1.16	5.38	1.90	4.77	7.30
Ge	1.21	6.07	2.01	4.60	7.53
Sn	1.40	7.7	1.96	4.30	7.05
Pb	1.44	6.8	2.33	3.90	7.82
H	0.32		2.2	7.18	
F	0.64		3.98	10.41	
Cl	0.99		3.16	8.30	
Br	1.14		2.96	7.59	
I	1.33		2.66	6.76	

<sup>a</sup> The covalent radii are from ref 47. The atomic polarizabilities are from ref 49. Estimated accuracies are 25% for Sn, and Pb, and 2% for C, Si, and Ge. The Pauling and ground state absolute electronegativities are from ref 45. The valence state  $sp^3$  (tetrahedral)  $\chi$  values for the M atoms in promoted state are from ref 52a.

electronegativity)<sup>45,50</sup> of carbon in group 14, compared to the other M atoms (see Table 1) explains the difficulty the halides have in stripping electrons away from that element (Figure 3). The situation for the most electronegative of the halides, X = F, is instructive; the (C  $\rightarrow$  F) charge shift,  $q_{F(M=C)}$ , is hardly two-thirds of the  $q_{F(M=C)}$  values obtained for the other M–F bonds (Figure 3b). For the other halides,  $q_{X(M=C)}$  are, of course, even less negative than  $q_{F(M=C)}$ . As we pointed out in a previous section, a net charge transfer from X to C (C  $\leftarrow$  X; so that  $q_X$  is actually positive) becomes increasingly likely going down group 17 from X = Cl to X = I (Figure 3b).

It is useful for our discussions to remind ourselves at this stage that the M atomic electronegativities,  $\chi$ , (and polarizabilities;<sup>50</sup> see Table 1) vary rather erratically going down group 14. On the Pauling scale ( $\chi^P$ ), C and Pb are the most electronegative elements in the group. Unfortunately, the Pauling and the ground state Mulliken (absolute) scales ( $\chi^{M(GS)}$ ) differ significantly on the electronegativity of Pb relative to the other elements in the group:<sup>51</sup> on the Mulliken scale,  $\chi^M$  decreases going down group 14 so that Pb is the least electronegative of all five elements.

Far better agreement with the Pauling scale is achieved, however, if we accept the Mulliken valence state (VS) electronegativities,  $\chi^{M(vS)}$ ,<sup>52</sup> (see the Appendix) rather than the ground state atomic  $\chi^M$  values (Table 1). These  $\chi^{M(vS)}$  values are specific to the  $sp^3$  (tetrahedral) hybridized state of the atoms, and concur

qualitatively with the  $\chi^P$  values that  $\chi(C) > \chi(Pb) > \chi(Si, Ge \text{ or } Sn)$  (cf.  $\chi^P$  and  $\chi^{M(vS)(tet)}$  in Table 1).

Indeed, a relatively high electronegativity of Pb is to be expected given the preferential stabilization of the s and p valence orbitals due to relativistic effects, which shows up even more prominently in other period 6 elements such as Pt, Au, and Hg.<sup>46</sup> Gold is, in fact, the most electronegative metal on both the Pauling and absolute electronegativity scales.<sup>45</sup>

Despite the rather small separation in the electronegativities of Pb and C, Pb is significantly more polarizable than C (Table 1). We see in the next sections that this observation is critical to understanding (i) why M  $\rightarrow$  X charge transfers in the haloplumbanes are so much larger than the charge transfers in the halomethanes (see Figure 3b), and (ii) the relative strengths of the X-bonds formed by both sets of molecules.

**3.2. Halogen Bonding and the Charge Distribution in  $MH_{4-n}X_n$  Molecules.** Several studies have confirmed a tendency for terminal chlorine, bromine, and iodine (X) atoms bonded to other atoms or groups (R–X) to form weak “noncovalent” bonds to electron rich sites (e.g., Y = F, O, N, or S) in neighboring molecules: R–X $\cdots$ Y–R'. These so-called halogen bonds arise from an electrostatic attraction between the Lewis base Y and a region of positive electrostatic potential (the  $\sigma$ -hole) on X outside the R–X overlap region. It is now well established that the size of the  $\sigma$ -hole and halogen bond strength increases as X becomes more polarizable: (F  $\ll$  Cl < Br < I).<sup>34</sup>

**3.2.1.  $\sigma$ -Hole and Orbital Hybridization at X.** A correlation has been identified in ref 34 between the size of the  $\sigma$ -hole and the extent of the %s composition of the X hybrid orbitals involved in the R–X bond, where R is a small organic fragment. In that work, Clark et al. showed that in the trifluorohalide molecules (F<sub>3</sub>C–X; X = F, Cl, Br, I) the increase in the size of the  $\sigma$ -hole going down group 17 (Cl < Br < I) correlates with a decrease in the %s composition of the X hybrid orbital in the C–X bond.<sup>34</sup> This observation is consistent with what we find for the halides in the  $CH_{4-n}X_n$  molecules. In Figure 4, the s participation in the X hybrid orbitals for M = C decreases continuously (for each n) going from the fluorides to the iodides (see the red M = C lines in Figure 4).

Beyond the halomethanes, we examine in this work the relationship between the halide orbital compositions (in Figure 4) and the propensity for halogen bonding in the Si, Ge, Sn, and Pb  $MH_{4-n}X_n$  molecules. Notice, for example, that in Figure 4 the s composition at X is always largest for M = Si (green lines), and is smallest, in almost all cases, when M = Pb (purple lines). Is this an indication that the halosilanes will be particular poor halogen bonding partners? Will the haloplumbanes form stronger halogen bonds than even the halomethanes? In con-

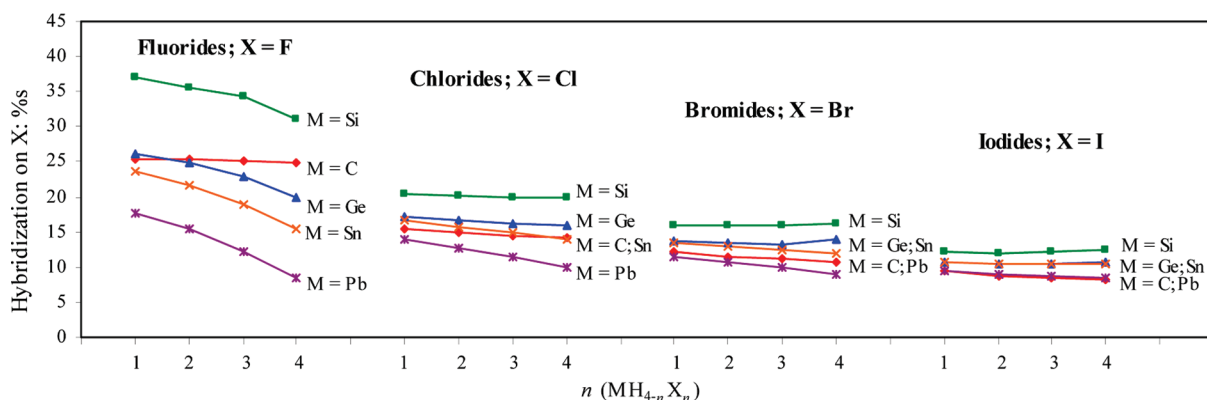


**Figure 4.** %s Contribution at X in the  $MH_{4-n}X_n$  Molecules.

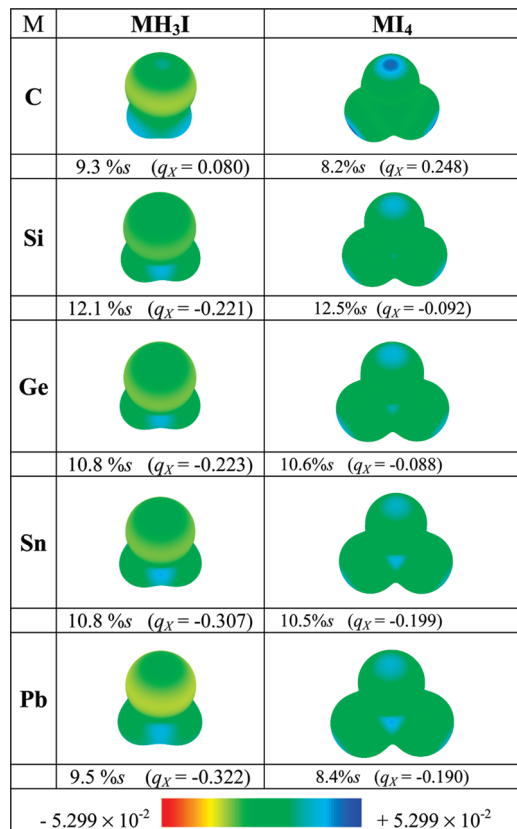


**Figure 5.** Electrostatic potentials in Hartree units on the 0.001 electrons/bohr<sup>3</sup> charge density isodensity surface of the group 14 MH<sub>3</sub>I and MI<sub>4</sub> molecules (M = C, Si, Ge, Sn, Pb). For valid comparisons, we use the same range for all the isodensity plots in this report.

fronting these and other questions about the nature of halogen bonding in the inorganic MH<sub>4-n</sub>I<sub>n</sub> systems, we use as our qualitative gauge the relative size and strength of the  $\sigma$ -holes on isodensity surfaces of the molecules.

**3.2.2. Dependence of the  $\sigma$ -Hole on M.** Interested in understanding better the influence of M on the  $\sigma$ -hole size and strength at the X substituents, we computed (i) the electrostatic potentials on the 0.001 electrons/bohr<sup>3</sup> isodensity surface of the iodo compounds, MH<sub>4-n</sub>I<sub>n</sub> ( $n = 1$ , and 4), and (ii) the hybridization at I in each of these systems.

We have focused our analysis on the iodides since the  $\sigma$ -holes are expected to be largest in these molecules (compared to the other halides). The electrostatic potentials for the two extreme cases in the MH<sub>4-n</sub>I<sub>n</sub> series ( $n = 1$  and 4), are shown in Figure 5. Our results confirm that, for each M, the  $\sigma$ -hole increases monotonously as  $n$  increases. Put another way, the MI<sub>4</sub> molecules are expected to form stronger halogen bonds than their less substituted MH<sub>4-n</sub>I<sub>n</sub> counterparts.

How does the size and strength of a  $\sigma$ -hole depend on M? As we mentioned before, replacing C by the softer or more polarizable Si, Ge, Sn, or Pb in MH<sub>4-n</sub>X<sub>n</sub> makes X far more negative (Figure 3b). So we anticipate that the  $\sigma$ -hole will be smaller and that the electrostatic potential will be less positive for M  $\neq$  C. This is exactly what we find if we compare the rows in Figure 5:  $q_I$  (for both the MH<sub>3</sub>I and the MI<sub>4</sub> systems) becomes substantially more negative, and the  $\sigma$ -hole is significantly attenuated when carbon is replaced by any of the heavier M atoms.

Interestingly, a comparison of the M = C and M  $\neq$  C cases in Figure 5 uncovers a rather strong correspondence between the charge at I,  $q_I$ , and the size of the  $\sigma$ -hole. Indeed, this

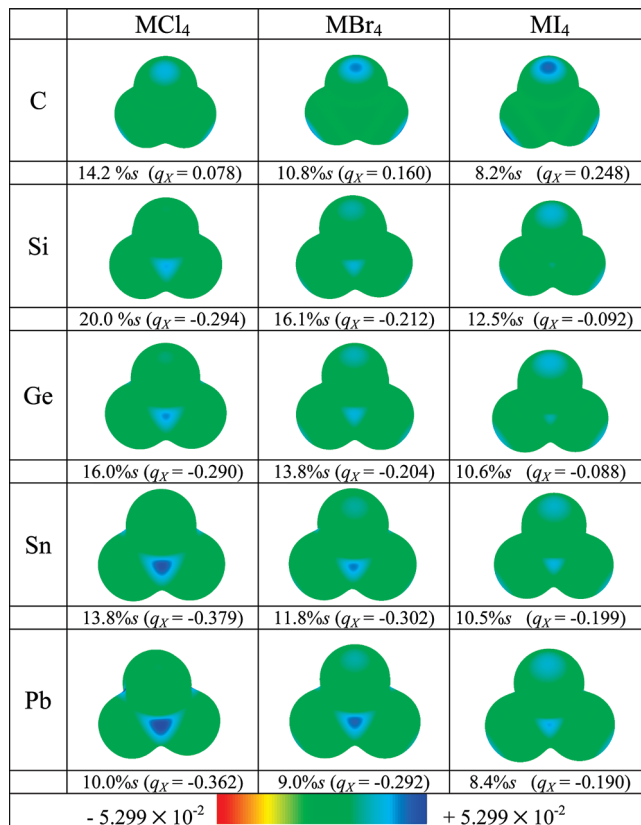


**Figure 6.** Plots of the electrostatic potentials in Hartree units on the 0.001 electrons/bohr<sup>3</sup> charge density isodensity surface of the group 14 MX<sub>4</sub> molecules (X = Cl, Br, I).

apparent link between  $q_I$  (see Figure 5) and the nature of the  $\sigma$ -hole is observed, as well, even when we compare the columns (MH<sub>3</sub>I vs MI<sub>4</sub>). In each case, the strengthening of the  $\sigma$ -hole going from the MH<sub>3</sub>I to the MI<sub>4</sub> systems is accompanied by (i) a definite positivation at I, and in several cases (ii) only an insignificant change in the %s composition at I.

These observations lead us to a few important guiding principles. (ia) For the less electronegative M atoms, the emergence of a  $\sigma$ -hole in the MH<sub>4-n</sub>X<sub>n</sub> molecules is better indicated by the changes in  $q_X$  rather than the %s compositions at X. The latter parameter changes rather insignificantly for Si, Ge, and Sn going from  $n = 1$  to  $n = 4$  (see Figure 4). (ib) The %s compositions at X is best utilized for M = C, or Pb. Perhaps more importantly, however, cross comparisons of the %s compositions at X (in CH<sub>4-n</sub>I<sub>n</sub> and PbH<sub>4-n</sub>I<sub>n</sub>, for example) can be quite misleading. Even though the hybridization at I is nearly identical for Cl<sub>4</sub> and PbI<sub>4</sub>, the  $\sigma$ -hole is clearly much stronger in Cl<sub>4</sub> than it is in PbI<sub>4</sub>. So, (ii), although the %s composition at X can be a good indicator of the relative significance of the  $\sigma$ -hole as a function of  $n$ , it is less reliable in cases where X is bonded to different M centers. In a later section, we examine further the reliability of both the X orbital compositions and  $q_X$  as relative measures of  $\sigma$ -hole strengths.

**3.2.3.  $\sigma$ -Hole and the Identity of X.** The expected increase in the size of the  $\sigma$ -hole going from CCl<sub>4</sub> to CBr<sub>4</sub> and Cl<sub>4</sub> is obvious going across each row in Figure 6. This is exactly the pattern that is anticipated by our discussion above and the work of Politzer et al.<sup>11,34</sup>

Going from M = C to M = Si, Ge, Sn, and Pb, the size and strength of the  $\sigma$ -hole (the intensity of the blue region at the top of the pictures in Figure 6) falls off rapidly. For the tetrachlorides, the  $\sigma$ -holes are obviously much weaker, for M

$\neq$  C. The holes become much more prominent for the  $\text{MBr}_4$  and  $\text{MI}_4$  molecules for all M, but remain strongest for the carbon compounds.

**3.2.4. Limitations in the Utility of %s Composition at X or  $q_X$  As Predictive Tools.** In a simple point charge model, an increase in the size and strength of the  $\sigma$ -hole at X may be associated a priori with an increase in the positive charge at X. Such a correspondence between the “positivation” at X and the nature of the  $\sigma$ -hole has been identified in a previous section for the iodomethanes,  $\text{MH}_{4-n}\text{I}_n$  (Figure 5). In those systems,  $q_1$  and the size of the  $\sigma$ -hole increases as  $n$  increases. In good agreement with Politzer et al. for  $\text{M} = \text{C}$ , however,<sup>11,17</sup> we have found that the extent of the %s composition at the X orbital can be a reliable indicator as well of how the  $\sigma$ -hole strength changes as a function of  $n$ , (across the rows for C and Pb in Figure 5) or as a function of X in  $\text{MX}_4$  (in Figure 6) for a given M.

It is now apparent from both Figures 5 and 6, however, that neither the %s compositions of the X hybrid orbital nor the magnitude of  $q_X$  is reliable as an indicator of how the  $\sigma$ -hole changes going from one M ( $= \text{C}, \text{Si}, \text{Ge}, \text{Sn}$  or  $\text{Pb}$ ) to another for a given  $\text{MH}_{4-n}\text{X}_n$  species. The %s composition at Cl in Figure 6, for instance, is lower in  $\text{SnCl}_4$  and  $\text{PbCl}_4$ , even though the  $\sigma$ -hole is most prominent in  $\text{CCl}_4$ . This limitation on the utility of the %s composition arises since the X hybrid orbital compositions can be quite insensitive (compared to the X atom orbital populations, and the  $\sigma$ -hole size) to the changes in size and polarizability going from one M center to another. Thus, for example, the %s compositions at I for  $\text{M} = \text{C}$  and  $\text{M} = \text{Pb}$  in column four of Figure 6 are almost identical even though the point charges ( $q_i$ ), and the electrostatic potentials at the  $\sigma$ -holes are quite different (cf. the surfaces for  $\text{CX}_4$  and  $\text{PbX}_4$  in Figure 6). Indeed, other indirect effects, such as changes in the X---X terminal atom separation (and repulsion) as M gets larger may also impact  $q_X$  (and the  $\sigma$ -hole, as well) more dramatically than they will the hybridization at X.

The trends (or lack thereof) in the orbital compositions and  $q_X$  going down Figures 5 and 6, have convinced us, therefore, that it is unadvisable to rely on either the X orbital hybridization or orbital populations in estimating how the  $\sigma$ -holes in molecules will evolve as a function of M. We want to emphasize, however, that both devices (the X orbital composition, and the point charge) appear to be somewhat more reliable as indicators of how  $\sigma$ -holes will change (expand and contract) as a function of  $n$  or X substituents for a fixed M.

**3.2.5.  $\sigma$ -Gap and the Nucleophilicity of M.** Let us mention briefly the gradual emergence of a conspicuous  $\sigma$ -gap (a prominent positive region) at the central (M) atoms in Figures 5, and 6.

In the halomethanes ( $\text{M} = \text{C}$ ), the electron density of the rather closely packed X atoms flows into the gaps and shroud the C nucleus sufficiently to enforce a more negative electrostatic potential in the center of the molecule. As M gets bigger, the halides get farther apart (going down the columns in Figure 6), so that the  $\sigma$ -gap becomes increasingly conspicuous and stronger (more positive). Indeed, such  $\sigma$ -gaps ( $\sigma$ -holes on the central atoms)<sup>28</sup> have been investigated for some halo-silanes and -germanes<sup>28,29</sup> and are identifiable on the surfaces of other (group 15) compounds as well.<sup>30</sup>

Notice that, for a given central atom, the size of the  $\sigma$ -gap decreases as X gets larger and less electron-withdrawing (going across the rows in Figure 6). The significance of the  $\sigma$ -gap is determined, evidently, by a balance between the ratio of the sizes of the M and X atoms and the difference in the

electronegativities of M and X. This observation is instructive for our understanding of the barriers to  $\text{S}_{\text{N}}2$  reactions at group 14 atoms in tetrahedral environments. Bickelhaupt and Bento<sup>53</sup> have confirmed, for example, that replacing C by Si in the simple halomethanes ( $\text{CH}_3\text{Cl}$ ) and other compounds alleviates the dense packing of the substituents (steric congestion) and diminishes the central barrier to  $\text{S}_{\text{N}}2$  reactions. They show, however, that if the Si center is bonded to even larger substituents, the central barrier emerges for Si compounds, too.<sup>53</sup> In the language we have adopted in this work; as M gets larger, the barrier to  $\text{S}_{\text{N}}2$  reactions will plummet, for a fixed set of substituents. This occurs for two reasons: (i) the M center becomes more positive (electrophilic; Figure 3a) and (ii) the  $\sigma$ -gap at the electrophilic M center gets larger and more accessible to the incoming nucleophile when C is replaced by any of the heavier group 14 congeners.

Indeed, our reference to a  $\sigma$ -gap at M on the iso-density surface is just another way to talk about a strengthening of the electrophilicity of the M center in the  $\text{MH}_{4-n}\text{X}_n$  compounds. The inferences we have made about the reactivity of M, based on the electrostatic potentials at the centers in Figures 5 and 6 are consistent with the general observations in refs 54 and 55. In those studies, the authors find that intra-<sup>54</sup> and intermolecular<sup>55</sup> nucleophilic attack at the group 14 atomic centers in their compounds becomes more favorable as M gets larger.

**3.3. Substituent Effects: A Closer Look.** Interested in improving our understanding of the relationship between the nature of the  $\sigma$ -hole at one terminal atom and the properties of the other (three) substituents bonded to a common M center, we compared the  $\sigma$ -holes at I in three different systems with the general formula  $\text{X}'_3\text{M-I}$ ; namely  $\text{H}_3\text{M-I}$  and  $\text{I}_3\text{M-I}$  and their fluoro- analogue,  $\text{F}_3\text{M-I}$ . The first two sets of systems ( $\text{X}' = \text{H}$  and  $\text{I}$ ) were discussed above in a different context. Here we consider the effects of a substitution in  $\text{X}'_3\text{M-I}$  for the radically more electronegative F alternative.

Clark et al. have shown that for the  $\text{H}_3\text{C-X---Y-R}$  halogen bonds (where  $\text{X} = \text{Cl}, \text{Br}$ , and  $\text{I}$ ), the strength of the  $\sigma$ -hole at X becomes significantly more positive, and the X-bond is strengthened when H is replaced by F atoms.<sup>34</sup> The situations for  $\text{M} = \text{Si}, \text{Ge}, \text{Sn}$  and  $\text{Pb}$  are considered here for the first time.

Our results for the  $\text{F}_3\text{M-I}$  systems in Figure 7 show that for each M the F substituents induce by far the largest and strongest  $\sigma$ -holes on the terminal iodide. More importantly, however, notice that the relative size and strength of the  $\sigma$ -hole as a function of M (going down Figure 7) is significantly substituent dependent. For  $\text{X}' = \text{H}$  or  $\text{I}$ , the  $\sigma$ -hole is relatively small and weak for  $\text{M} = \text{Si}, \text{Ge}, \text{Sn}$ , and  $\text{Pb}$  compared to the carbon systems at the top of the figure. This is the same trend highlighted previously in reference to Figure 6 as well (which also includes the cases for X,  $\text{X}' = \text{Cl}$ , and  $\text{Br}$ ). For  $\text{X}' = \text{F}$ , however, the situation is quite different: The  $\sigma$ -holes are far smaller and apparently weaker for both  $\text{CF}_3\text{I}$ , and  $\text{SiF}_3\text{I}$  than they are for  $\text{GeF}_3\text{I}$ ,  $\text{SnF}_3\text{I}$ , and  $\text{PbF}_3\text{I}$ .

We can draw a few key conclusions from the result in Figure 7. For the  $\text{X}'_3\text{M-I}$  molecules (for any M) the  $\sigma$ -hole gets larger as the substituent,  $\text{X}'$ , gets more electronegative (going across each row). However, we find that the extent of the M-mediated “through bond” perturbation of the  $\sigma$ -hole by  $\text{X}'$  may be far more dramatic for one M compared to another. In Figure 7, we see, for example, that the  $\sigma$ -hole at I in  $\text{X}'\text{M-I}$  (i) shrinks if we replace C by Sn or Pb in one case (e.g., when  $\text{X}' = \text{I}$ ), but (ii) expands dramatically in another case (when  $\text{X}' = \text{F}$ ). So, it is, in fact, rather difficult to predict whether replacing C in any

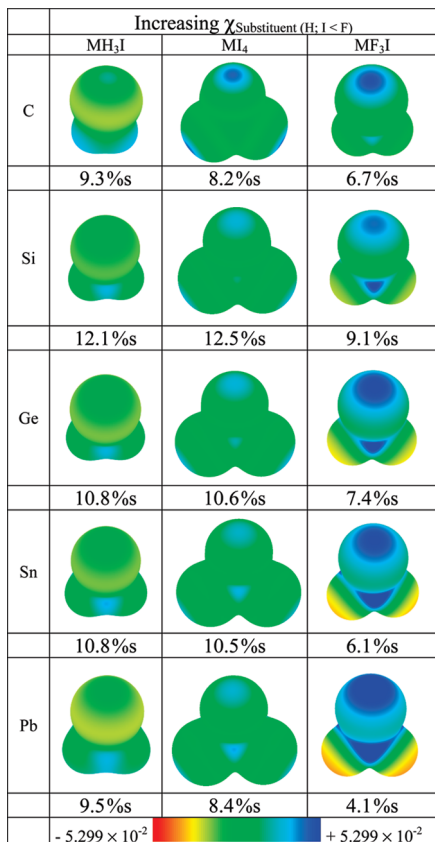


**Figure 7.** Plots of the electrostatic potentials in Hartree units on the 0.001 electrons/bohr<sup>3</sup> charge density isodensity surface of the X'<sub>3</sub>M-I molecules (X' = H, I and F). The columns are arranged according to the (Pauling) electronegativities of X'.

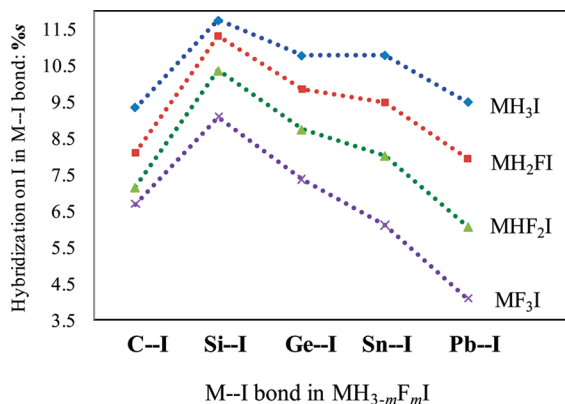


**Figure 8.** Hybridization (% *s* composition) of the I orbitals in the M-I bond in the four MH<sub>3-*m*</sub>F<sub>*m*</sub>I molecules (*m* = 0, 1, 2, and 3). The change in the %*s* composition,  $|\Delta\%s|$ , from *m* = 0 to *m* = 3 are 2.5% (C); 3.0% (Si); 3.4% (Ge); 4.7% (Sn); 5.4% (Pb).

arbitrary halogen bonded (X'<sub>3</sub>C-I---Lewis Base) complex by M = Si, Ge, Sn or Pb will strength or weaken the X-bond. The effect of replacing C will depend not only on the identity of M, but will rely to a very significant extent on the identity of X'.

**3.3.1. X Hybridization Data and Nuances in the Substituent Effects.** The complete set of %*s* orbital composition data for I in all the mixed (iodo-fluoro) halides MH<sub>3-*m*</sub>F<sub>*m*</sub>I molecules (*m* = 0, 1, 2, 3) are plotted in Figure 8. We pointed out previously that the changes in the %*s* compositions of the X hybrid orbital going down group 14 from one M to another is an unreliable predictor of how the corresponding  $\sigma$ -hole changes as function of M. This is partly because identically hybridized orbitals bonded to different M atoms may have vastly different popula-

tions. For any given M-X bond, however, a decrease (increase) in the %*s* composition in the X hybrid orbital does correspond to some degree of enlargement (contraction) of the  $\sigma$ -hole. A comparison of the sizes of the  $\sigma$ -holes in, for example, MH<sub>3</sub>I and MF<sub>3</sub>I in Figure 7 and the X hybrid orbital compositions in Figure 8 is instructive, enabling us, in fact, to better appreciate the dependence of the  $\sigma$ -hole profile on M and the X' substituents.

Notice that, in Figure 8, the %*s* composition at X in the M-X bond is highest for MH<sub>3</sub>I for each M. As the H atoms are replaced by F atoms the effect is to decrease the %*s* composition at X and to increase the  $\sigma$  hole size and strength (see Figure 7). Notice too, however, that as *m* increases in Figure 8, the decrease in the %*s* composition is disproportionately large for M = Sn and Pb. Going from *m* = 0 to *m* = 3, the %*s* compositions at I are  $|\Delta\%s|$  = 4.7 and 5.4%, for Sn and Pb, respectively, compared to  $|\Delta\%s|$  = 2.5 and 3.0%, for C and Si, respectively. This explains the massive expansion of the  $\sigma$ -hole in the Sn and Pb compounds going from X' = H to X' = F at I in Figure 7.

Why, though, are the F substituents far more successful in inducing a reduction in the %*s* composition at I when bonded to Sn or Pb than they are when bonded to C? A qualitative argument from polarization provides us with the most convincing rationale for this substituent effect. An increase in the number of the very polarizing F substituents causes an increase in the electron withdrawing power of the -MH<sub>3-*m*</sub>F<sub>*m*</sub> fragment for all M. The change is necessarily more dramatic, however, for the more polarizable M atoms (see Table 1); hence, the massive expansion of the  $\sigma$ -hole at I for M = Ge, Sn, and Pb (comparing columns 2 and 4 in Figure 7).

Taken together, the  $\sigma$ -hole pictures and the orbital hybridization data in Figures 7 and 8 provide us with substantial evidence that (i) increasing the number of electronegative (polarizing) substituents will strengthen the X-bonds; and will do so most radically for the most polarizable central atoms. So, for a given Lewis base, although (ii) the X-bond to CH<sub>3</sub>I is expected to be far stronger than the X-bond to SnH<sub>3</sub>I or PbH<sub>3</sub>I, (iii) the X-bond to SnF<sub>3</sub>I or PbF<sub>3</sub>I will be comparable to or even stronger than those to CF<sub>3</sub>I.

In the broadest terms, our results indicate that for any given set of X' substituents, the ordering of the X'<sub>3</sub>M-I---NH<sub>3</sub> X-bond energies, for example, (for M going from C to Pb) cannot be predicted simply from the properties of the M atoms. The relative strength of the halogen bonds has a complicated dependence on both the number and the identity of the X' substituents as well.

To quantify the dependence of the X-bonds on substituents, we have determined the actual I---N interaction energies for the series of group 14 MH<sub>3</sub>I and MF<sub>3</sub>I compounds halogen bonded to NH<sub>3</sub> molecules as shown in Table 2.<sup>56</sup> The interaction energies of all the complexes, E(X'<sub>3</sub>M-I---NH<sub>3</sub>), has been corrected for basis set superposition errors (BSSEs) using the counterpoise correction strategy as implemented in ref 38. The results conform in important ways to the patterns that are already evident from the  $\sigma$ -hole and hybridization data in Figures 7 and 8. Among the hydrides, the H<sub>3</sub>C-I---NH<sub>3</sub> complex has the shortest and strongest halogen bond; the interaction energies fall off quite rapidly in fact as the M atoms get larger. The interaction energy is an order of magnitude weaker for the Pb system ( $\Delta E$  = -0.24 kcal·mol<sup>-1</sup>) compared to the C case ( $\Delta E$  = -1.69 kcal·mol<sup>-1</sup>)

The strengths of all the X-bonds jump significantly when we substitute for the fluorine atoms: increasing by just over ~2 to



**TABLE 2: BSSE Corrected H<sub>3</sub>M–I---NH<sub>3</sub> and F<sub>3</sub>M–I---NH<sub>3</sub> Halogen-Bonding Interaction Energies<sup>a</sup>**

complex	I–N, Å	$\Delta E^b$ , kcal·mol <sup>-1</sup>
H <sub>3</sub> C–I–NH <sub>3</sub>	<b>3.082</b> (3.071) <sup>c</sup>	<b>-1.69</b> (-2.5) <sup>c</sup>
H <sub>3</sub> Si–I–NH <sub>3</sub>	3.304	-0.90
H <sub>3</sub> Ge–I–NH <sub>3</sub>	3.262	-0.79
H <sub>3</sub> Sn–I–NH <sub>3</sub>	3.299	-0.51
H <sub>3</sub> Pb–I–NH <sub>3</sub>	3.270	-0.24
F <sub>3</sub> C–I–NH <sub>3</sub>	2.894(2.882) <sup>c</sup>	-5.09(-6.4) <sup>c</sup>
F <sub>3</sub> Si–I–NH <sub>3</sub>	3.160	-3.23
F <sub>3</sub> Ge–I–NH <sub>3</sub>	2.998	-4.93
F <sub>3</sub> Sn–I–NH <sub>3</sub>	2.986	-4.90
F <sub>3</sub> Pb–I–NH <sub>3</sub>	<b>2.713</b>	<b>-8.28</b>

<sup>a</sup>  $\Delta E = E(\text{Complex}) - (E(\text{NH}_3) + E(\text{MX}_3\text{I}))$  where  $X' = \text{H, F}$ . The shortest I---N bond distance and largest energy for both the hydride and fluoride series are in bold. <sup>b</sup> This work. <sup>c</sup> BSSE corrected (BP86/DZVP) computational data from ref 56.

2.6 fold (for M = C, and Si) and by 5.3, 8.6, and 33.0 fold for M = Ge, Sn, and Pb. These impressive increases in  $\Delta E$  for Ge, Sn, and for Pb in particular, are accompanied by significant reductions in the I---N distances for  $X' = \text{F}$  (Table 2). In the case of the F<sub>3</sub>Pb–I---NH<sub>3</sub> system, not only is the bond distance severely shortened (by 0.56 Å, relative to the PbH<sub>3</sub>I case), the F<sub>3</sub>Pb–I---NH<sub>3</sub> X-bond is the strongest of all those listed in the series, exceeding the interaction energy for the F<sub>3</sub>C–I---NH<sub>3</sub> complex by over 3.0 kcal·mol<sup>-1</sup>.

For the GeX<sub>3</sub>I and SnX<sub>3</sub>I systems, the interaction energies increase so dramatically when we substitute for the F atoms that the  $\Delta E$  values become comparable with  $\Delta E$  for the F<sub>3</sub>C–I case (cf.  $\Delta E$  for the hydrides and fluorides in Table 2). Among the MF<sub>3</sub>I complexes, it is the Si system that has the longest and the weakest bond. These important outcomes for  $\Delta E$  are, of course, quite gratifying, since they are (qualitatively) precisely what one expects, given the small change in the %s contribution for I going from SiH<sub>3</sub>I to SiF<sub>3</sub>I (cf. the blue and purple lines in Figure 8) compared to the (noticeably larger) rehybridizations at I in Ge, Sn, and Pb cases.

Several entailments follow from the patterns that have emerged in this section. As we mentioned in the introduction, various instances of halogen bonding to C–X sites in molecules have already been identified and exploited. Our results demonstrate that these interactions may be strengthened (or attenuated) significantly by the selective replacements of C centers by the heavier Si, Ge, Sn, and Pb congeners, where (e.g., biological or industrial) applications permit. These X-bond interactions may be further fine-tuned by a strategic selection of the number and type of substituents; each factor (M, n and X') playing strong yet interdependent roles in determining the stability of halogen bonds.

**3.4. Summary and Outlook.** Theoretical investigations of the basic nature of halogen bonding to date have tended to focus on small halogenated organic molecules.<sup>11,34</sup> The heavier analogues of the halomethanes have been largely ignored, even as interest in the chemistry of heavy analogues of organic compounds continues to grow. In this paper, we have examined in detail the charge distribution in 100 halomethanes and their heavier group 14 analogues and the evolution of the  $\sigma$ -hole at X as a function of M and the number and nature of other substituents.

We report the first systematic investigation of the nature of the  $\sigma$ -hole at halide sites in the Si, Ge, Sn, and Pb analogues of halomethanes. In agreement with the results of Politzer et al. for the M = C,<sup>11,34</sup> we find that the %s composition at the X orbital in the M–X bond is a reliable indicator of the relative

size and strength of the  $\sigma$ -hole in some MH<sub>4–n</sub>X<sub>n</sub> systems, but is limited as a gauge for how the  $\sigma$ -hole will change when X is bonded to different M centers.

The propensity for halogen bonding in a given organic compound may be significantly altered we find by replacing the C center to which X is bonded with one of the heavier group 14 elements. The more polarizing the X' substituents are in the X'<sub>3</sub>M–I molecules, and the more polarizable M is, the larger the  $\sigma$ -hole becomes, and, ultimately, the stronger the halogen bond will be. Of the 100 molecules considered in this work, F<sub>3</sub>Pb–I (and not F<sub>3</sub>C–I, for instance) is expected to form the strongest linear halogen bonds to simple Lewis bases.

Halogen bonding continues to find applications and to attract investigation into its fundamental properties as well.<sup>12,23,24</sup> Our results for the Ge, Sn, and Pb systems in particular invite even further exploration of the phenomenon of halogen bonding in inorganic halides.

## Appendix

**Valence State Electronegativities and the Positive Charges at I in MH<sub>4–n</sub>I<sub>n</sub>.** In a short series of papers,<sup>52</sup> Bratsch provided a comprehensive list of Mulliken (Absolute) Electronegativities for atoms in molecules. He obtained these atomic valence state (sp, sp<sup>2</sup>, sp<sup>3</sup>, etc.) electronegativities by taking linear sums of the weighted s and p orbital contributions to the valence state promotion energies. These energies were then used to obtain valence state ionization energies, IE<sub>v</sub>, and electron affinities, EA<sub>v</sub>, (from the corresponding ground state values: IE<sub>G</sub>, and EA<sub>G</sub>). The valence state Mulliken electronegativities were computed following the familiar form of the (Mulliken) definition of electronegativity:

$$\chi^{M(\text{vs})} = \frac{\text{IE}_v + \text{EA}_v}{2}$$

A list of the VS specific electronegativities for the central M atoms in a tetrahedral coordination is included in Table 1. For this discussion we consider only the ground state values for the terminal hydrogen and halogen atoms.

Notice that although the ground state Mulliken electronegativity of iodine,  $\chi(\text{I})$ , is larger than the ground state value for carbon (Table 1), the valence state sp<sup>3</sup> (tetrahedral) electronegativity of carbon is significantly larger than  $\chi(\text{I})$ . This implies that the rehybridization at the roughly sp<sup>3</sup> carbon in the CH<sub>4–n</sub>I<sub>n</sub> molecules may create a situation in which  $\chi^{\text{VS}}$  for the hybridized carbon exceeds  $\chi(\text{I})$ , thus enforcing the observed C<sup>–</sup>–I<sup>+</sup> polarity in these systems (see Figure 3a,b).

This observation, and the  $\chi^{\text{VS}}$  values in Table 1, help us to rationalize the positivation at many of the Cl and Br in the chloro- and bromomethanes as well (see Figure 3b). Given the  $\chi^{\text{VS}}$  values in Table 1, we would expect, indeed, as is observed in Figure 3b, that the  $q_X$  values are small for X = Cl since  $\chi_{\text{C}}^{\text{VS}} \approx \chi_{\text{Cl}}^{\text{GS}}$ , and positive  $q_X$  for X = Br and I since  $\chi_{\text{C}}^{\text{VS}} > \chi_{\text{Br}}^{\text{GS}}$  and  $\chi_{\text{I}}^{\text{GS}}$ .

**Acknowledgment.** This research was supported by awards from Research Corporation (Cottrell College Science Award No. 7742) and from the Thomas F. and Kate Miller Jeffress Memorial Trust (Award J-903). We thank the University of Richmond for the award of a (Chemistry Department) Puryear-Topham research fellowship to B.K.W., and Arts and Sciences research fellowships to B.K.W. and C.C. Carol

Parish is thanked for helpful discussions and for reading a draft of the manuscript.

**Supporting Information Available:** MP2(full) and experimental geometrical data for the  $\text{CH}_{4-n}\text{X}_n$ ,  $\text{SiH}_{4-n}\text{X}_n$ ,  $\text{GeH}_{4-n}\text{X}_n$ ,  $\text{SnH}_{4-n}\text{X}_n$ , and  $\text{PbH}_{4-n}\text{X}_n$  molecules ( $X = \text{F}, \text{Cl}, \text{Br}, \text{and I}$ ), NBO point charges, and M and X orbital hybridizations (%s compositions) for all  $\text{MH}_{4-n}\text{X}_n$  compounds ( $M = \text{C}, \text{Si}, \text{Ge}, \text{Sn}, \text{and Pb}$ , and  $X = \text{F}, \text{Cl}, \text{Br}, \text{and I}$ ). This material is available free of charge via the Internet at <http://pubs.acs.org>.

## References and Notes

- (1) Greenwood, N. N.; Earnshaw, A. *Chemistry of the Elements*, 2nd ed.; Elsevier Butterworth-Heinemann: Oxford, 2005. See Chapter 10, in particular, section 10.2.4, p. 373ff for some of the differences in the chemical reactivity of the elements and the (in)stability of some compounds. See also the tables on pp 372 and 373.
- (2) See, for example, p 339; section 10.3.1 pp 374–375 in ref 1.
- (a) Waltenburg, H. N.; Yates, J. T., Jr. *Chem. Rev.* **1995**, *95*, 1589.  
(b) Section 9.3.3, pp 340–342 in ref 1.
- (4) Vanhellefont, J.; Simoen, E. *J. Electrochem. Soc.* **2007**, *154*, H572.
- (5) See sections 10.3.1, pp 374–375, and 10.3.2, pp 381–382, 385 in ref 1.
- (6) Donald, K. J.; Böhm, M. C.; Lindner, H. J. *J. Mol. Struct. Theochem* **2004**, *710*, 1.
- (7) Donald, K. J.; Böhm, M. C.; Lindner, H. J. *J. Mol. Struct. Theochem* **2005**, *713*, 215.
- (8) See refs 6 and 7. We determined that the lengthening of the M–X bond as  $n$  increases is caused by a competition between the M–X attraction and the X–X repulsions around the small carbon center for the large Cl and Br terminal atoms.
- (9) (a) Carpenter, J. E.; Weinhold, F. *J. Mol. Struct. Theochem* **1988**, *169*, 41. (b) Reed, A. E.; Curtiss, L. A.; Weinhold, F. *Chem. Rev.*, **1988**, *88*, 899, and references therein.
- (10) Metrangolo, P.; Neukirch, H.; Pilati, T.; Resnati, G. *Acc. Chem. Res.* **2005**, *38*, 386.
- (11) Politzer, P.; Lane, P.; Concha, M. C.; Ma, Y.; Murray, J. S. *J. Mol. Model.* **2007**, *13*, 305.
- (12) Libri, S.; Jasim, N. A.; Perutz, R. N.; Brammer, L. *J. Am. Chem. Soc.* **2008**, *130*, 7842.
- (13) In a halogen bond (R–X–Y–R'), the halide, X, is bonded to some moderately to very electron withdrawing group R. The group electronegativity of R determines how substantial the shift in the electron density along the bond axis—away from X and toward R—will be.
- (14) See: (a) Politzer, P.; Murray, J. S.; Concha, M. C. *J. Mol. Model.* **2007**, *13*, 643. (b) Wang, Y.-H.; Lu, Y.-X.; Zou, J.-W.; Yu, Q.-S. *Int. J. Quantum Chem.* **2008**, *108*, 1083.
- (15) (a) Dumas, J. M.; Peurichard, H.; Gomel, M. *J. Chem. Res., Synopses* **1978**, *2*, 54. (b) In ref 11, Politzer et al. suggests that the term “halogen bond” was first used in ref 15a. We have not been able to find any earlier use of the term.
- (16) Legon, A. C. *Angew. Chem., Int. Ed.* **1999**, *38*, 2686.
- (17) (a) Politzer, P.; Murray, J. S.; Lane, P. *Int. J. Quantum Chem.* **2007**, *107*, 3046. (b) Voth, A. R.; Khuu, P.; Oishi, K.; Ho, P. S. *Nature Chem.* **2009**, *1*, 74.
- (18) Hassel, O. *Science* **1970**, *170*, 497.
- (19) Bent, H. A. *Chem. Rev.* **1968**, *68*, 587.
- (20) (a) Ramasubbu, N.; Parthasarathy, R.; Murray-Rust, P. *J. Am. Chem. Soc.* **1986**, *108*, 4308. (b) Lommerse, J. P. M.; Stone, A. J.; Taylor, R.; Allen, F. H. *J. Am. Chem. Soc.* **1996**, *118*, 3108.
- (21) Lu, Y.; Shi, T.; Wang, Y.; Yang, H.; Yan, X.; Luo, X.; Jiang, H.; Zhu, W. *J. Med. Chem.* **2009**, *52*, 2854.
- (22) (a) Auffinger, P.; Hays, F. A.; Westhof, E.; Ho, P. S. *Proc. Natl. Acad. Sci. U.S.A.* **2004**, *101*, 16789. (b) Voth, A. R.; Hays, F. A.; Ho, P. S. *Proc. Natl. Acad. Sci. U.S.A.* **2007**, *104*, 6188.
- (23) (a) Metrangolo, P.; Resnati, G. *Chem.—Eur. J.* **2001**, *7*, 2511. (b) Bilewicz, E.; Rybarczyk-Pirek, A. J.; Dubis, A. T.; Grabowski, S. J. *J. Mol. Struct.* **2007**, *829*, 208. (c) Fourmigué, M. *Curr. Opin. Solid State Mater. Sci.* **2009**, *13*, 36.
- (24) Espallargas, G. M.; Zordan, F.; Marín, L. A.; Adams, H.; Shankland, K.; van de Streek, J.; Brammer, L. *Chem.—Eur. J.* **2009**, *15*, 7554.
- (25) Brinck, T.; Murray, J. S.; Politzer, P. *Int. J. Quant. Chem. (Quant. Biol. Symp.)* **1992**, *19*, 57.
- (26) We use the term “strength” instead of electrophilicity to refer to the positive electrostatic potential (ESP) within the  $\sigma$ -hole. The  $\sigma$ -hole gets stronger as the ESP gets more positive.
- (27) Politzer, P.; Murray, J. S. An Overview of  $\sigma$ -Hole Bonding, an Important and Widely-Occurring Noncovalent Interaction. In *Practical Aspects of Computational Chemistry Methods, Concepts, and Applications*; Leszczynski, J., Shukla, M. K. Eds.; Springer: Heidelberg, 2009; Ch. 6.
- (28) Murray, J. S.; Lane, P.; Politzer, P. *J. Mol. Model.* **2009**, *15*, 723.
- (29) Politzer, P.; Murray, J. S.; Lane, P.; Concha, M. C. *Int. J. Quantum Chem.* **2009**, *109*, 3773.
- (30) Murray, J. S.; Lane, P.; Politzer, P. *Int. J. Quantum Chem.* **2007**, *107*, 2286.
- (31) Murray, J. S.; Lane, P.; Clark, T.; Politzer, P. *J. Mol. Model.* **2007**, *13*, 1033.
- (32) Politzer, P.; Murray, J. S.; Concha, M. C. *J. Mol. Model.* **2008**, *14*, 659. See also refs 5–13 therein. As this reference emphasizes, halogen bonding depends on the variation in the charge distribution (hence the magnitude and sign of the electrostatic potential) across the surface of X atoms in molecules. This critical level of detail is sacrificed in point charge models.
- (33) Even if X in the acid/base pair R–X–Y–R' has a noticeable local  $\sigma$ -hole (outside the bonding region; see Figure 1) it is still possible for X to have a net (global) negative charge if, in the bonding region, the R → X charge transfer is significant. Now, since Y is necessarily an electron-rich site, it would have a net negative charge as well. Thus, a simple point charge model would predict, incorrectly, that the interaction between X and Y is always repulsive, independent of the R–X–Y bond angle. See ref 32.
- (34) Clark, T.; Hennemann, M.; Murray, J. S.; Politzer, P. *J. Mol. Model.* **2007**, *13*, 291.
- (35) Head-Gordon, M.; Head-Gordon, T. *Chem. Phys. Lett.* **1994**, *220*, 122, and references therein.
- (36) (a) Krishnan, R.; Binkley, J. S.; Seeger, R.; Pople, J. A. *J. Chem. Phys.* **1980**, *72*, 650. (b) McLean, A. D.; Chandler, G. S. *J. Chem. Phys.* **1980**, *72*, 5639.
- (37) (a) Peterson, K. A. *J. Chem. Phys.* **2003**, *119*, 11099 (for Sn and Pb). (b) Peterson, K. A.; Shepler, B. C.; Figgen, D.; Stoll, H. *J. Phys. Chem. A* **2006**, *110*, 13877 (for I). The correlation consistent triple-zeta (cc-pVTZ-pp) basis sets used are from the website of the Institute for Theoretical Chemistry at the University of Stuttgart: <http://www.theochem.uni-stuttgart.de/pseudopotentials/clickpse.en.html>.
- (38) Frisch, M. J.; Trucks, G. W.; Schlegel, H. B.; Scuseria, G. E.; Robb, M. A.; Cheeseman, J. R.; Montgomery, J. A., Jr.; Vreven, T.; Kudin, K. N.; Burant, J. C.; Millam, J. M.; Iyengar, S. S.; Tomasi, J.; Barone, V.; Mennucci, B.; Cossi, M.; Scalmani, G.; Rega, N.; Petersson, G. A.; Nakatsuji, H.; Hada, M.; Ehara, M.; Toyota, K.; Fukuda, R.; Hasegawa, J.; Ishida, M.; Nakajima, T.; Honda, Y.; Kitao, O.; Nakai, H.; Klene, M.; Li, X.; Knox, J. E.; Hratchian, H. P.; Cross, J. B.; Bakken, V.; Adamo, C.; Jaramillo, J.; Gomperts, R.; Stratmann, R. E.; Yazyev, O.; Austin, A. J.; Cammi, R.; Pomelli, C.; Ochterski, J. W.; Ayala, P. Y.; Morokuma, K.; Voth, G. A.; Salvador, P.; Dannenberg, J. J.; Zakrzewski, V. G.; Dapprich, S.; Daniels, A. D.; Strain, M. C.; Farkas, O.; Malick, D. K.; Rabuck, A. D.; Raghavachari, K.; Foresman, J. B.; Ortiz, J. V.; Cui, Q.; Baboul, A. G.; Clifford, S.; Cioslowski, J.; Stefanov, B. B.; Liu, G.; Liashenko, A.; Piskorz, P.; Komaromi, I.; Martin, R. L.; Fox, D. J.; Keith, T.; Al-Laham, M. A.; Peng, C. Y.; Nanayakkara, A.; Challacombe, M.; Gill, P. M. W.; Johnson, B.; Chen, W.; Wong, M. W.; Gonzalez, C.; Pople, J. A. *Gaussian 03, Revision E.01*; Gaussian, Inc.: Pittsburgh PA, 2003.
- (39) The GaussView (3.0 and 4.1) graphics program has been used to plot the representations of the electrostatic potentials in this report.
- (40) Graner, G.; Hirota, E.; Iijima, T.; Kuchitsu, K.; Ramsay, D. A.; Vogt, J.; Vogt, N. In *Landolt-Börnstein - Numerical Data and Functional Relationships in Science and Technology; Group II: Molecules and Radicals Volume 25. Structure Data of Free Polyatomic Molecules, Sub-volume A: Inorganic Molecules*. Martienssen, W., Kuchitsu, K., Eds., Springer-Verlag: Berlin, Heidelberg, 2006.
- (41) (a) Fujii, H.; Kimura, M. *Bull. Chem. Soc. Jpn.* **1970**, *43*, 1933. (b) Wolf, S. N.; Krisher, L. C.; Gsell, R. A. *J. Chem. Phys.* **1971**, *54*, 4605. (c) Bürger, H.; Betzel, M.; Schulz, P. *J. Mol. Spectrosc.* **1987**, *121*, 218. (d) Haaland, A.; Hammel, A.; Martinsen, K.-G.; Tremmel, J.; Volden, H. V. *J. Chem. Soc.: Dalton Trans.* **1992**, 2209.
- (42) (a) Results obtained at the MP2 level for the halomethanes, and their silicon and germanium analogues have been presented and discussed in detail in parts 1 and 2 of the series. Small differences have been observed between the geometrical and other MP2(full) data from this work for C, Si, and Ge (shown in the supporting information) and the data available in the preceding papers in the series. (b) See ref 43.
- (43) (a) Lewars, E. G. *Computational Chemistry: Introduction to the Theory and Applications of Molecular and Quantum Mechanics*, Kluwer Academic Publishers: Norwell, MA, 2004; pp 231–241. (b) In contrast to the less expensive MP2 method, the MP2(full) method takes all the core electrons into account in assessing the contributions of the doubly excited state to the total energy of the system.
- (44) The general contraction in the M–X bond distance as  $n$  increases has been highlighted and discussed in ref 7 for several of the  $\text{MH}_{4-n}\text{X}_n$  molecules:  $\text{CH}_{4-n}\text{X}_n$ ,  $\text{SiH}_{4-n}\text{X}_n$ , and  $\text{GeH}_{4-n}\text{X}_n$  ( $X = \text{F}, \text{Cl}, \text{and Br}$ ). See ref 8.
- (45) Emsley, J. *The Elements*, 3rd Ed.; Clarendon Press: Oxford, 1998.

(46) (a) Pyykkö, P. *Adv. Quantum Chem.* **1978**, *11*, 353. (b) Pyykkö, P. *Chem. Rev.* **1988**, *88*, 563.

(47) Pyykkö, P.; Atsumi, M. *Chem.—Eur. J.* **2009**, *15*, 186.

(48) The relatively smaller changes in the atomic radii after silicon are explained by the well known d-orbital and lanthanide contractions (after period three, and from periods five (Sn) to six (Pb), respectively). For Pb, relativistic effects are responsible for a contraction of the valence s and p orbitals, as well.

(49) *CRC Handbook of Chemistry and Physics*, 87th ed.; Lide, D. R., Ed.; CRC Press: Boca Raton, FL, 2006–2007.

(50) Although atomic electronegativities are not quantum mechanical observables, they remain indispensable and chemically meaningful tools for discussions of the charge distributions in molecules. For a detailed discussion of a relationship between atomic polarizabilities and Pauling electronegativities. See: Nagle, J. K. *J. Am. Chem. Soc.* **1990**, *112*, 4741.

(51) For Si, Ge, and Sn, the Pauling (as well as the Mulliken (absolute)) electronegativities are quite close:  $\chi^P = 1.90, 2.01$  and  $1.96$ , respectively (Table 1), but Si is the least electronegative element in the series. On the (ground state, Mulliken) absolute scale, Pb is the least electronegative element in the group ( $\chi_{\text{Pb}}^P = 3.90$  eV; Table 1).

(52) (a) Bratsch, S. G. *J. Chem. Educ.* **1988**, *65*, 34. (b) Bratsch, S. G. *J. Chem. Educ.* **1988**, *65*, 223.

(53) Bento, A. P.; Bickelhaupt, F. M. *J. Org. Chem.* **2007**, *72*, 2201.

(54) Beuter, M.; Kolb, U.; Zickgraf, A.; Bräu, E.; Bletz, M.; Dräger, M. *Polyhedron* **1997**, *16*, 4005.

(55) Bento, A. P.; Bickelhaupt, F. M. *Chem. Asian J.* **2008**, *3*, 1783.

(56) Valerio, G.; Raos, G.; Meille, S. V.; Metrangolo, P.; Resnati, G. *J. Phys. Chem. A* **2000**, *104*, 1617.

JP102856V